Available online at www.eccomasproceedia.org
Eccomas Proceedia COMPDYN (2023) 97-111

ECCOMAS
Proceedia

COMPDYN 2023
9th ECCOMAS Thematic Conference on
Computational Methods in Structural Dynamics and Earthquake Engineering
M. Papadrakakis, M. Fragiadakis (eds.)
Athens, Greece, 12-14 June 2023

DEVELOPMENT OF A TUNED LIQUID PARTICLE DAMPER WITH OPTIMISED DAMPING CHARACTERISTICS

Sebastian Völkel[1], **Kersten Latz**[1]

[1]Department of Civil Engineering, University of Applied Sciences Wismar
23966 Wismar, Germany
e-mail: {sebastian.voelkel, kersten.latz}@hs-wismar.de

Abstract. *For slender structures with horizontal vibration amplitude under earthquakes or strong wind loads, pendulum dampers are usually the preferred solution. However, these dampers have the disadvantage that the entire system with pendulum and damper is a technically complex and expensive construction, and for structures with low natural frequencies, the pendulums need a lot of space due to their length. One alternative is the Tuned Liquid Sloshing Damper (TLSD). The advantage of the lower technical effort is offset by the disadvantages of non-adjustable damping and wave breaking at large deflections. To increase the effectiveness, it is necessary to further develop the TLSD so that the degree of damping can be precisely adjusted and the non-linear behaviour can be avoided. This can be optimised as follows: Floating pellets on the liquid surface ensure that energy is extracted from the system and the sloshing movements of the liquid through internal friction and wall friction subside more quickly. The optimal level of damping can be precisely adjusted via the quantity of particles and other parameters. With an additional lightweight rigid plate placed above the pellets, the surface of the fluid-particle filling can be forced to move almost linearly.*

Keywords: Vibration damper, Tuned Liquid Sloshing Damper, Tuned Liquid Particle Damper, Structural control, Slender structures.

ISSN:2623-3347 © 2023 The Authors. Published by Eccomas Proceedia.
Peer-review under responsibility of the organizing committee of COMPDYN 2023.
doi: 10.7712/120123.10390.21085

1 INTRODUCTION

Slender structures such as wind turbines, towers, high-rise buildings and long-span pedestrian bridges are often sensitive to dynamic actions due to earthquakes and wind and have shown considerable vibration amplitudes in a horizontal direction. The response behaviour of these structures is considered critical especially when the frequency spectra of the acting loads overlap with the structure's natural frequencies. As a rule, the lowest building frequencies can lead to critical response behaviour and resonance vibrations. As the spectrum of impacts cannot usually be influenced, there are essentially four ways to improve this resonant behaviour:

(a) Increase of the lowest structure natural frequencies by stiffening

(b) Improvement of damping behaviour

(c) Vibration isolation

(d) Installation of a vibration damper

Stiffening the structure can only be achieved economically by reducing the slenderness of the structure, which in many cases is not possible from a structural point of view. The increase of structural damping can be realised primarily by using energy-dissipating elements between an external fixed point and the structure[1, 2]. The effect of measures restricted to the support area is limited in the case of bridges and wind turbines. Measures for active and passive vibration isolation are understood to be the shielding of the excitation forces from the building. While in active vibration isolation, these measures are to be taken directly at the generator, in passive isolation the building is shielded from the environment by spring elements and, if necessary, also damping elements. Isolating measures are not applicable if the forces act directly on the building. In many applications, the last option is to install a vibration damper. This possible entails the coupling of a spring-mass system which is designed in such a way that the response behaviour is minimised in the event of excitation at the critical system's natural frequency. However, due to this additional degree of freedom, two new natural frequencies occur above and below the original system frequency. By implementing a tuned mass damper, an ideal frequency response curve can be generated in which resonance phenomena are no longer detectable in the range of the corresponding natural frequency.
The problem-adapted degree of damping is essential for the effectiveness of a vibration damper. Too much damping would lead to significant system responses in the range of the original natural frequency. If the degree of damping is below the optimum, resonance phenomena will occur within the range of the two new frequencies. An optimisation criterion for the degree of damping for harmonic force excitation was developed by Den Hartog in 1940 [3]. The technical implementation of the vibration damper can be carried out with these four different systems:

(a) Spring-mass damper

(b) Pendulum damper

(c) Frahm tank

(d) Sloshing damper

While systems (a) and (c) can limit vertical vibrations, as can be observed in bridges, sports grandstands and ceilings, systems (b) and (d) act in a horizontal direction. Pendulum dampers are used in particular for slender high-rise buildings. To realise the optimum degree of damping, elaborate viscous dampers must be provided. As a result, these vibration dampers take up a lot of space and are relatively expensive. The sloshing damper is an alternative that has been used comparatively rarely up to now. When the liquid in the container is excited to slosh, restoring forces – similar to the spring-mass system – occur which lead to a weakly damped sloshing movement of the fluids. The advantage of the low technical complexity of the sloshing damper is offset by the disadvantages of the non-adjustable damping and the wave breaking at large deflections. This turbulent movement leads to non-linear vibration behaviour and contradicts the effect of a vibration damper.

2 Development of the Tuned Liquid Particle Damper (TLPD)

To increase the effectiveness, it is necessary to further develop the sloshing dampers in such a way that the degree of damping can be precisely adjusted and a breaking wave is avoided at large deflections. For the range of amplitudes in which an unbroken surface wave is present, the mechanical model of a two-mass oscillator is valid [4]. In the linear range, a portion of the fluid does not participate in the sloshing motion. The passive mass is attributed to the generalised mass m_1 of the main system. A model developed as early as 1952 by Graham and Rodriguez [5] is described in [4] and the functions for determining the active $m_{12,a,n}$ and passive mass $m_{12,p}$ of a rectangular vessel are given.

$$\frac{m_{12,a,n}}{m_{12}} = \frac{8tanh[(2n-1)\pi\lambda]}{\pi^3(2n-1)^3\lambda} \tag{1}$$

with:
$\lambda = h_{12}/L$ =Filling level/sloshing length
$n = 1$ for the 1st natural frequency, 2 for the 2nd natural frequency, etc.

$$\frac{m_{12,p}}{m_{12}} = 1 - \sum_{n=1}^{\infty} \frac{m_{12,a,n}}{m_{12}} \tag{2}$$

The optimal coupling stiffness $c_{12,opt}$ and damping $d_{12,opt}$ between the main mass and the active damper mass required to minimise the amplitudes of the vibration path of a two-mass vibrator can be calculated according to Den Hartog [3, 6] for the first natural frequency under harmonic force excitation as a function of the modal mass ratio μ.

$$\mu = \frac{m_{12,a,n}}{m_1 + m_{12,p}} \tag{3}$$

$$\frac{\omega_1}{\omega_{12,opt}} = \frac{1}{1+\mu} \tag{4}$$

$$c_{12,opt} = (2\pi\omega_{12,opt})^2 m_{12} \tag{5}$$

$$d_{12,opt} = \sqrt{\frac{3\mu}{8(1+\mu)^3}} 2\, m_{12}\, \omega_1 \tag{6}$$

In the case of a horizontal movement of a partially filled rectangular tank, according to [7] the angular frequency of the sloshing function of the free surface can be described by a Fourier series for each eigenmode:

$$\omega_{\omega,ij} = \sqrt{gk_{ij}tanh(k_{ij}h)} \tag{7}$$

$$k_{ij} = \pi\sqrt{(i/L_1)^2 + (j/L_2)^2} \tag{8}$$

$$i + j \neq 0$$

where g is the acceleration due to gravity, k_{ij} is the eigenmode, L_1 and L_2 are the horizontal dimensions of the tank in two directions and h is the filling level. The surface profile, associated with the eigenmodes, can be described by the following equation:

$$\eta(x,y) = cos[i\pi(x + \frac{1}{2}L_1)/L_1]cos[j\pi(y + \frac{1}{2}L_2)/L2] \tag{9}$$

$$i, j \leq 0$$

If only the two-dimensional behaviour of the container is to be considered, then $L_2 = \infty$ and the equation will simplify to:

$$\omega_{\omega,ij} = \sqrt{gk_itanh(k_ih)} \tag{10}$$

$$k_{ij} = \pi i/L_1 \tag{11}$$

The solution for calculating the sloshing frequency of further tank geometries is given in [8, 9]. To increase the damping in the TLSD and to approach the optimum, flow-obstructing components are usually added to the damper. Approaches and mathematical methods for the design of the dampers can be found in [10, 11, 12].

2.1 Adding pellets to TLSD

Another way to extract energy from the TLSD is by adding floatable pellets to the surface of the fluid. Internal friction and wall friction ensure that energy is extracted from the system and the sloshing movements of the liquid quickly subside. The optimal damping level of the Tuned Liquid Particle Damper (TLPD) can be precisely configured via the number of particles. In the series of experiments, expanded polystyrene pellets with a diameter of 25 mm were introduced in layers as shown in Fig. 1. The more pellets added, the higher the damping of the system.

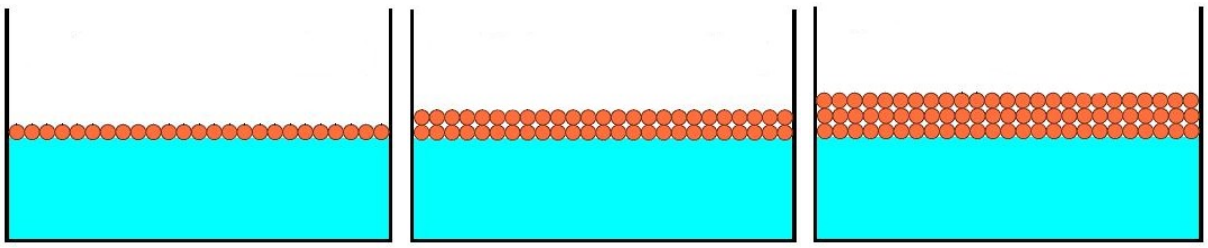

(a) (b) (c)

Figure 1: Pellet rows for adjusting the damping decay

2.2 Adding a lightweight rigid plate

In the case of a tank partially filled with water, a movement of the free surface occurs when the tank is excited horizontally, as described in section 2.0. Depending on the size of the excitation, the dimensions of the tank and the physical properties of the liquid, the movement can take on any sloshing form from linear, to discontinuous, to turbulent [7]. With an additional lightweight rigid plate floating above the pellets, as shown in Fig. 2(a)(c), the surface of the fluid-particle filling can be forced to move almost linearly. Higher sloshing eigenmodes of the fluids are suppressed and thus non-linear effects are significantly reduced. The series of experiments showed that the damping of the system can only be increased to a limited extent by adding the pellets. By ballasting the plate as shown in Fig. 2(b) compression of the pellets can be achieved. This results in increased internal friction, thus further increasing the damping of the system and enabling it to be configured more precisely. If the ballasting takes place in the rotation axis of the bending-resistant plate, this leads to a minimal influence on the sloshing frequency of the system with simultaneous uniform compression of the pellets over the entire plate surface.

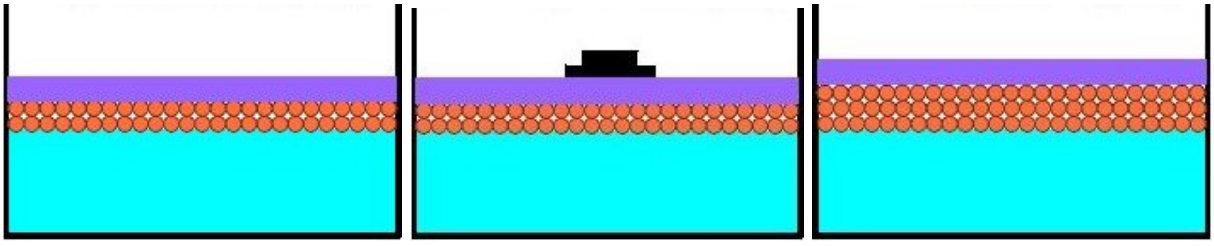

(a) (b) (c)

Figure 2: Pellet rows, lightweight rigid plate and additional weight

3 Shaking table experiments

The determination of the damping of the different configurations of the TLPD and the control of the calculated sloshing frequency was done by performing free vibration tests on a shaker table. The basin, which is fixed on a movable carriage, is excited by a horizontal movement tuned to the first sloshing frequency. By recording and evaluating the decay of the sloshing amplitudes, the damping and frequency of the tested damper configurations can be determined.

3.1 Experimental setup

The shaker table shown in Fig. 3 consists of a horizontally movable carriage mounted on linear bearings and an electric motor that can be controlled in the RPM range. The rotation of the motor is transformed by a crankshaft into a uniform horizontal movement of the slide. When the motor is at rest, the carriage can be assumed to be rigid. The water basin to be analysed, made of float glass, is firmly mounted on the movable carriage. After determining the sloshing frequency to be achieved, the basin is filled with water up to the corresponding filling level (10) and the various configurations of floatable pellets, bending-resistant plate and additional mass are installed. In the first series of experiments, the damping behaviour of a tank with dimensions L =1150 mm W =300 mm and h_0 =200 mm was investigated. The calculated expected value (10) of the first sloshing frequency in the longitudinal direction of the container is 0.581 Hz.

The course of the decaying oscillation is recorded with the aid of a level probe PSENSE320 from Driesen + Kern GmbH. The level probe measures the relative pressure change of the water level in comparison to the resting water level at the edge of the tank over the decay period at a sampling frequency of 10 Hz. The evaluation of the measurement data of the sloshing frequency ω_d and the damping coefficient δ was carried out by polynomial curve-fitting based on the corresponding homogeneous solution of the free damped oscillation (12) for the case $r(t) = 0$ with the initial conditions $x(t = 0) = x_0$ and $\dot{x}(t = 0) = v_0$ and the measurement data over the time range of the free vibration decay process using non-linear regression analysis.

$$x_h(t) = e^{-\delta t}[x_0 cos(\omega_d t) + \frac{v_0 + \delta x_0}{\omega_d} sin(\omega_d t)] \tag{12}$$

For the test rig, described below in section 4, a second series of tests was carried out. Here, a container with the dimensions L =438 mm W =438 mm and h_0 =110 mm was fixed on the described shaker table and an optimal system configuration was sought by varying the pellet quantity and the additional mass. The measurement data collection of the free vibration decay curve was carried out by measuring the vertical displacement of the rigid plate at the edge of the container over the time range of the vibration decay. A CCD laser displacement measuring system LK-G507 from Keyence was used as the sensor. Compared to the level probe, the laser sensor allows a higher sampling frequency of 100 Hz, with simultaneously improved repeatability and linearity of the measurement.

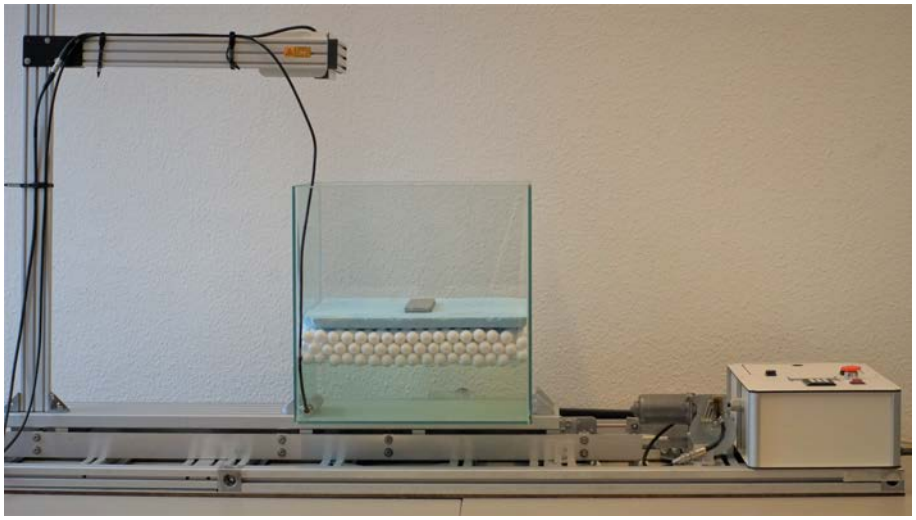

Figure 3: Experimental setup shaking table

3.2 Results

After evaluating the vibration decay curves for the different system configurations of the first test series, it can be seen in Fig. 4 that the expected value of the sloshing frequency is reached almost independently of the number of pellets and the additional mass. The results of the damping determination are shown for 0, 2 and 4 layers of pellets. In addition to the data points given as a function of the varying mass, a linear trend line is shown for the respective data series and the associated upper and lower 95% confidence interval. When increasing the ballast without the use of pellets, a small increase in damping from $D = 1.20\%$ (0 g additional weight) to $D = 2.10\%$ (3000 g additional weight) can be observed. If two layers of pellets are

added to the system, damping values between $D = 2.60\%$ to $D = 5.50\%$ can be achieved. If the amount of pellet mass is doubled further, damping values of the system between $D = 3.50\%$ and $D = 7.10\%$ can be achieved, depending on the additional weight.

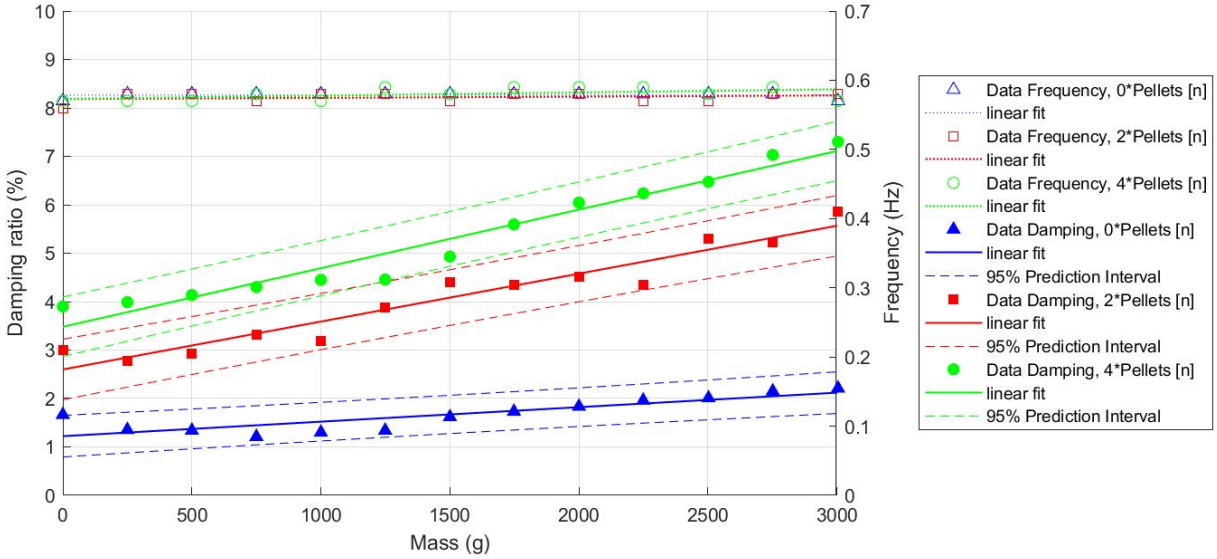

Figure 4: Damping and frequency related to the additional mass

The second series of experiments is limited to the determination of the optimal system configuration for the test stand from section 4. The expected value for the sloshing frequency of the basin is 1.04 Hz (5)(10), the damping ratio should reach $D = 11.38\%$ (6). The test series was conducted with 217 g of pellets. At an additional load of 500 g, Fig. 5(a), a sloshing frequency of 1.05 Hz and a damping ratio of $D = 10.08\%$ was achieved. The second analysed damper configuration was equipped with an additional mass on the rigid plate of 750 g. In this configuration, a sloshing frequency of 1.05 Hz and a damping ratio of $D = 13.04\%$ was achieved in the analysis, Fig. 5(b). Linear interpolation between the two results yields the optimum damping ratio at an additional mass of 595 g.

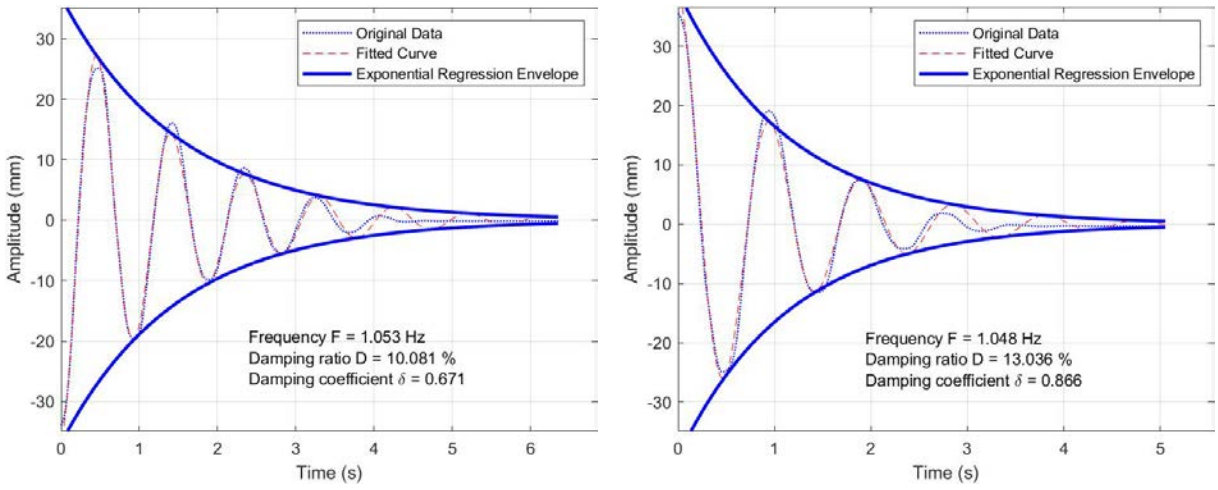

(a) mass=500g (b) mass=750g

Figure 5: Damping tank dimensions L =438mm, h_0 =110mm, pel=217g pel size=25mm

4 TLPD-structure interaction

It makes sense to test the efficiency and functionality of a newly developed damper on a real structure. As part of the project, a 10.00 m high test tower was built, the parameters of which can be taken from Table 1. The first natural frequency of this tower is 1.08 Hz, which is in the same range as the lowest natural frequencies of small wind turbines and chimneys. Free vibration tests as well as tests with harmonic excitation were carried out on this tower.

4.1 Experimental setup

The base plate of the test tower is rigidly connected using 16 anchor rods on a reinforced concrete foundation with the dimensions $L = 2.60$ m, $B = 2.60$ m and $H = 0.80$ m. At the top of the tower, a two-storey test platform made of square tubes with the dimensions $L = 1.35$ m, $B = 0.60$ m and $H = 0.60$ m is mounted. As shown in Fig. 6, a Shaker BD5 from Wölfel Engineering GmbH can be placed on the lower level, in addition to extra masses for fine-tuning the first natural frequency of the tower. The shaker, which is equipped with an electrodynamic linear drive, enables the tower to be excited in a targeted manner in the frequency range from 0.5 Hz to 200 Hz with a controllable excitation force of 20 N to 500 N in the horizontal direction. The upper level offers the option to assemble and test prototypes of the TLPD.

(a) Front view (b) Test platform

Figure 6: Experimental setup testing tower

To determine the damping behaviour of the tower, free vibration tests were carried out:

(a) Without TLSD

(b) With TLSD

(c) With TLPD

In experiments (b)(c), the container described in section 3.1 in the second series of experiments was used. For experiment (c), 217 g of pellets and 595 g of additional mass were added to the tank. The damper configuration is summarised in Table 1. To create the horizontal deflection, a low-stretch rope was attached between an earth anchor and the tower at a height of 10 m.
Using an angle of attack of 45 degrees, the rope was pre-tensioned to 700 N. The resulting horizontal deflection of the tower due to the pretension was 26 mm. Afterwards, the fixation was abruptly released and the horizontal acceleration of the tower during the free vibration decay was recorded by an acceleration sensor of the type B12\200 of the company Hottinger Brüel & Kjaer GmbH fixed to the mast with a measuring interval of 20 Hz. The damping of the test configurations is evaluated with a polynomial curve fitting over the maxima and minima of the amplitudes of the decay process using non-linear regression analysis for the function of the decay curve (13).

$$x_h(t) = C\, e^{-\delta t} \tag{13}$$

To check the frequency response and the tuning of the damper, a test was carried out using a frequency sweep for the test configuration from the free vibration tests (a),(b) and (c). The shaker attached to the test platform excited the tower in a frequency range from 0.6 Hz to 1.6 Hz with a force of 30 N for a time period of 300 s. The horizontal acceleration of the tower is recorded by the accelerometer throughout excitation. The recorded accelerations are transferred into the frequency range using Fast Fourier Transformation for the evaluation of the experiment.

System	Property	Symbol	Unit	Value
Structure	Height	H	[m]	10.0
	Tube dimension	D	[mm]	219.1 x 8
	Mode shape	n	[-]	1
	Eigenfrequency	f_1	[Hz]	1.08
	Generalised modal mass	m_1	[kg]	404.97
	Damping ratio	D_1	[%]	0.14
TLPD	Number of TLPD units	N	[-]	1
	Length	L	[mm]	438
	Width	W	[mm]	438
	Resting water height	h_0	[mm]	110
	Frequency	f_{12}	[Hz]	1.04
	Amount of pellets	n	[g]	217
	Plate mass	m_{Pl}	[g]	189
	Additional mass	m_A	[g]	595
	Water mass	m_{12}	[kg]	21.10
	Active mass	$m_{12,a}$	[kg]	14.89
	Damping ratio	D_{12}	[%]	11.38

Table 1: Parameter testing tower and TLPD

4.2 Results

The measurement data of the horizontal accelerations at the tower head for the free vibration tests are shown for the test series (a) without TLSD, (b) with TLSD and (c) with TLPD in Fig. 7. At time 0 s, the fixation of the preload was abruptly released and the free vibration decay process was initiated. The damping of the tower without a damper is $D = 0.14\%$. By mounting a TLSD, the damping could be increased to $D = 0.95\%$. The interference between the harmonic oscillation of the damper and the tower is noticeable. The deviation of the first maximum and minimum amplitudes from the decay curve can be explained by a breaking wave and a resulting increased energy dissipation. The non-linear effect caused by the decay curve was not taken into account in the curve fitting to determine the system damping. By optimally adjusting the damping to the system, the damping of the entire system could be further increased to $D = 6.48\%$.

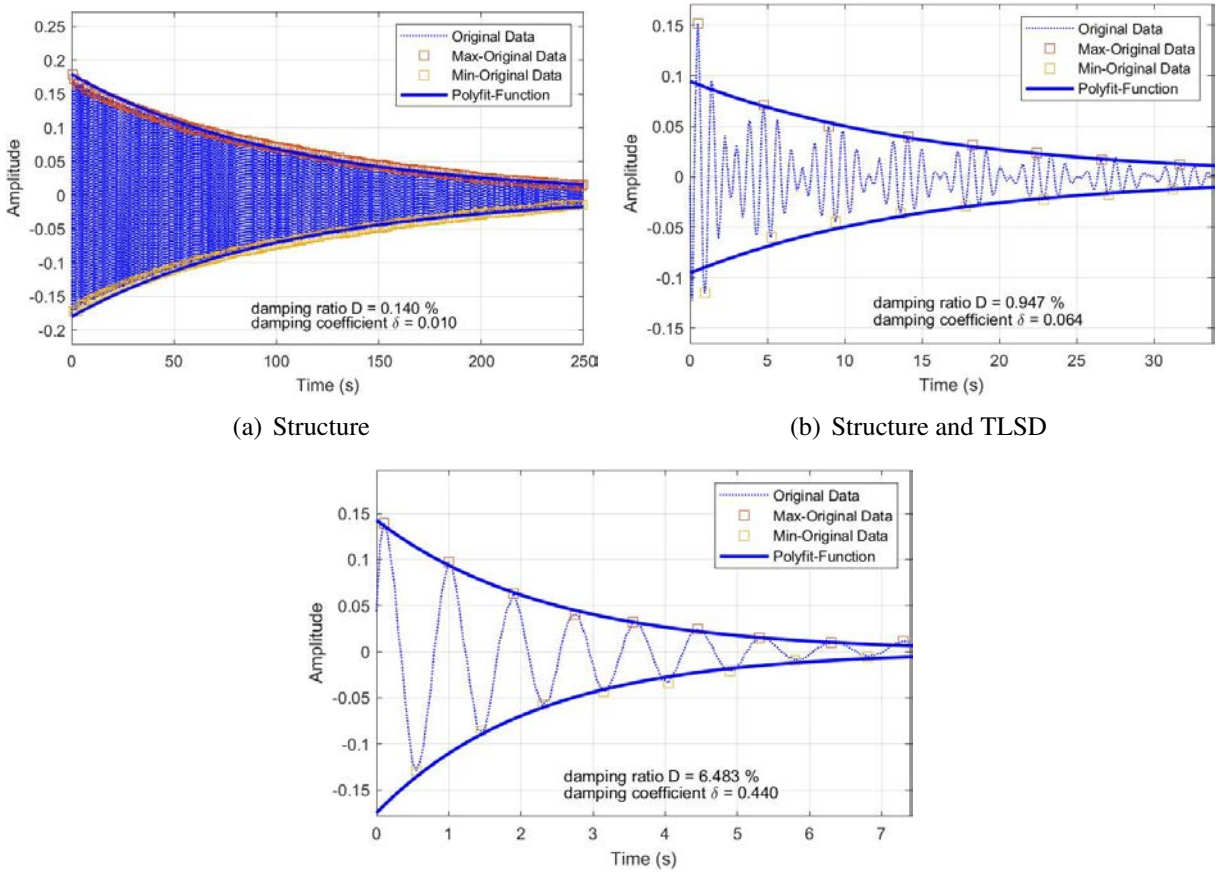

(a) Structure

(b) Structure and TLSD

(c) Structure and TLPD

Figure 7: Free vibration tests on the testing tower

The horizontal acceleration measured during the harmonic force excitation by the shaker has been transferred from the time domain to the frequency domain. In Fig. 8, the results for the system configuration without TLSD, with TLSD, and with TLPD are shown. The comparison between the analytically solved damped two-mass oscillator with the applied system parameters of the test rig (a) and the collected measured values (b) shows a very good agreement of the maximum amplitudes of the component response over the frequency range of the excitation. In

the tuning ratio range from 1.15 to 1.4, a deviation between the measured data and the expected value can be seen. During the steady state of the system, problems arise with the control of the shakers' excitation unit due to the large amplitudes and the low stiffness of the tower.

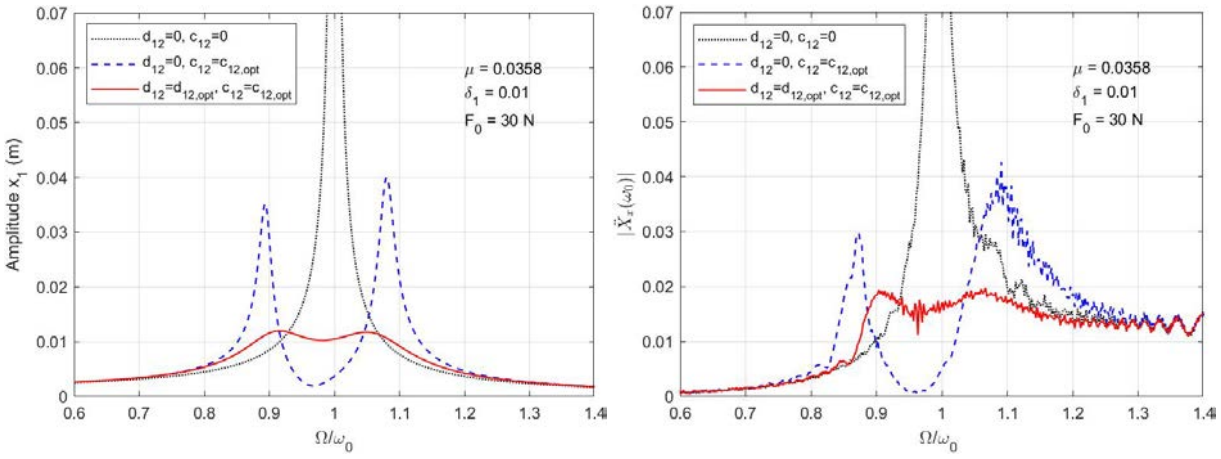

(a) Expected values (b) Measurement

Figure 8: System response testing tower

5 Application example on a small wind turbine

The system presented can be used well as a tuned damper for wind turbines. For example, a TLPD was developed for a small wind turbine with a vertical axis shown in Fig. 9 (a). If the centre of gravity of the rotor is not exactly at the intersection of the axis of rotation, harmonic excitation will occur during the rotation of the blades. The dynamic amplitude resulting from this is largely dependent on the structural damping. Without additional dampers, the system can't be operated at a rotational speed range that matches the first natural frequency. Currently, operations in the critical speed range can be avoided by controlling the rotational speed. With a TLPD, the critical speed range can be reduced and thus the efficiency of the system can be increased.

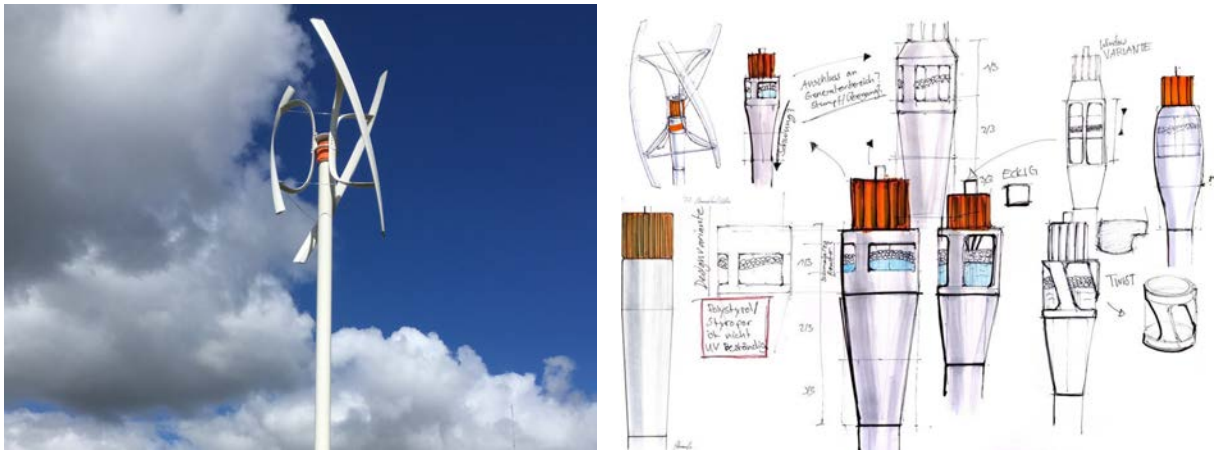

(a) Without TLPD (b) Design approach of the integration of the TLPD [13]

Figure 9: Wind turbine with vertical axis

The directional sinusoidal horizontal force due to the unbalance of the rotor F results from the mass of the rotor m_u, the eccentricity of the rotor r_u and the angular frequency of the operating speed Ω:

$$F = m_u r_u \Omega^2 sin\Omega t \tag{14}$$

The vibration equation of the system is:

$$m\ddot{x} + d\dot{x} + kx = m_u r_o \Omega^2 sin\Omega t \tag{15}$$

$$\ddot{x} + 2D\omega_0\dot{x} + \omega_0^2 x = \epsilon\, \Omega^2 sin\Omega t \tag{16}$$

$$\epsilon = r_u \frac{m_u}{m} \tag{17}$$

As a pure sinusoidal oscillation with phase shift, the stationary oscillation path results from the unbalance excitation for the steady state:

$$x(t) = \hat{x} sin(\Omega t + \varphi) \tag{18}$$

$$\eta = \frac{\Omega}{\omega_0} \tag{19}$$

$$\hat{x} = \epsilon \frac{\eta^2}{\sqrt{(1-\eta^2)^2(2D\eta^2)}} \tag{20}$$

$$\varphi = arctan\left(\frac{-2D\eta}{1-\eta^2}\right) \tag{21}$$

If the magnification function of the system is defined as the dynamic amplitude $\hat{x}$ by the eccentricity ϵ, the function results:

$$V_4(\eta, D) = V_3(\eta, D) = \frac{\hat{x}}{\epsilon} = \frac{\eta^2}{\sqrt{(1-\eta^2)^2 + (2D\eta)^2}} \tag{22}$$

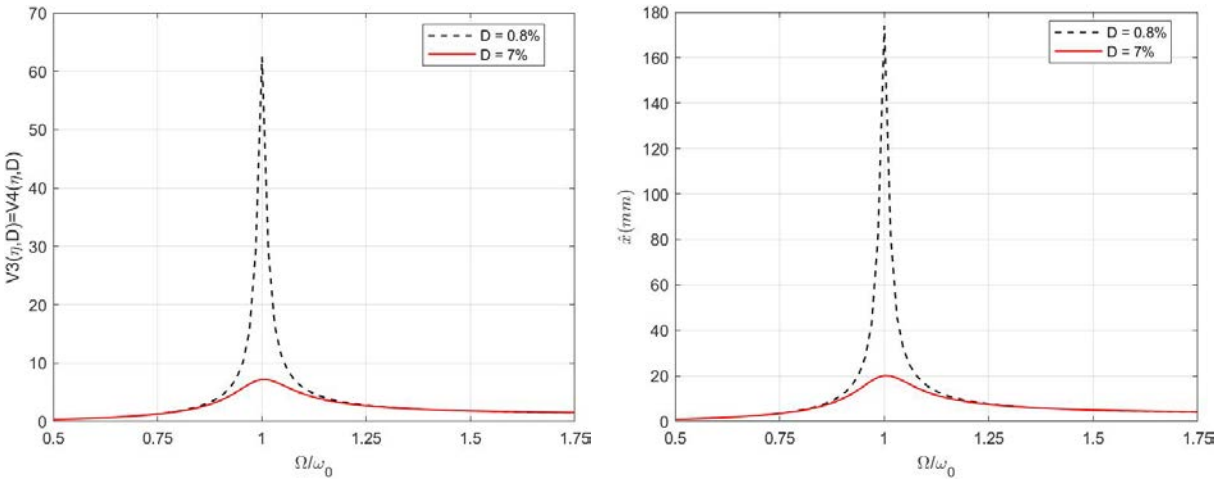

(a) Magnification function (b) Dynamic amplitude

Figure 10: Steady state response

In Fig. 10 (a) the magnification function $\frac{\hat{x}}{\epsilon}$ over the tuning ratio is shown for a system with a mass eccentricity r_u =9.375 mm, a rotor mass m_u =562 kg and a modal mass m =1889.42 kg for a damping ratio of 0.8% without damper and 7% with damper. Figure 10 (b) shows the resulting dynamic amplitude $\hat{x}$ concerning the tuning ratio. The realisable damping of 7% can reduce the dynamic amplitudes from 175 mm without TLPD to 20 mm with TLPD. Fig. 9 (b) shows the TLPD integrated into the upper area of the mast [13]. It is designed to be circular in shape, allowing easy cable routing from the generator to the base of the system inside the mast. It is possible to determine the optimum damper frequency according to (6) and (10). The necessary dimensions of the TLPD are determined by the sloshing frequency of a circular ring according to [8]:

$$\omega_{mn}^2 = \frac{g}{R_a}\xi_{mn} tanh\left(\frac{\xi_{mn} h}{R_a}\right) \tag{23}$$

with g the acceleration due to gravity, h the filling height, R_a the outer radius and ξ_{mn} as the positive roots of the equation $\Delta_m(\xi_{mn} = 0)$. The results for ξ_{mn} for different values depending on the radius ratio $k = \frac{R_i}{R_a}$ for the first slosh eigenmode are given by [9] in Table 2.

k	0.1	0.2	0.3	0.4	0.5	0.6	0.7	0.8	0.9
n=0	1.8035	1.7051	1.5821	1.4618	1.3537	1.2621	1.1824	1.1134	1.0531

Table 2: Roots of the determinant $\Delta_m(\xi_{mn}) = 0$ for different values of radii ratio k

For the system shown in Fig. 9, (23) gives a TLPD with dimensions R_a = 0.3175 m, R_i = 0.0325 m and a filling height of h =0.2 m. The expected value of the sloshing frequency is f_{12} =1.07 Hz. The damping of the TLPD is to be set to a damping ratio of 10.5 %. A prototype of the circular ring, shown in Fig. 11 (a), was made using a 3D printer and swing-out tests were carried out on the shaker table.

(a) Prototype annular tank

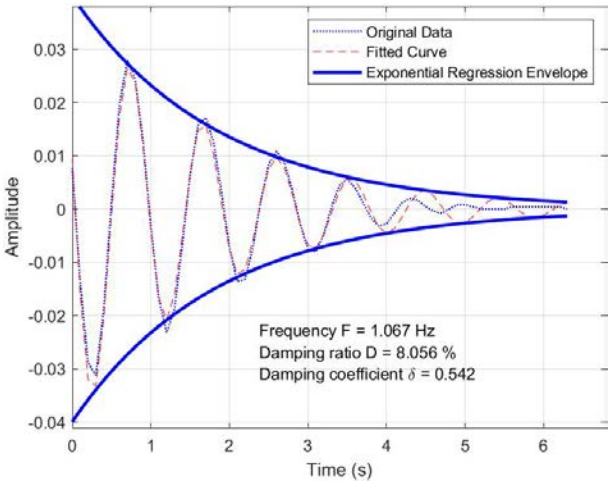

(b) Result free vibration decay

Figure 11: Free vibration test on shaking table for annular tank

Fig. 11 (b) shows the result of the first free vibration decay test. The expected values of the frequency could be achieved in a first test with 4 layers of pellets and 1000 g additional mass. The damping of 8% is still below the expected value. An increase in the damping with an increase in the additional mass is to be expected.

6 Concluding Remarks

A detailed investigation of the further development of the TLSD was carried out. In free vibration tests of the sloshing motion of the damper configurations, the linear increase of the damping as a function of the pellet quantity and the additional weight could be shown. The TLPD provides two parameters for the precise adjustment of the damping dimension D: The number of pellets and the ballasting of the rigid plate with the accompanying compression of the underlying pellet rows. If the additional mass is arranged in the rotation axis of the lightweight plate, the sloshing frequency remains constant. The rigid plate also suppresses higher sloshing eigenforms and reduces the non-linear effects of the sloshing motion. To test the effectiveness and functionality of the TLPD, a test tower was harmonically excited by a frequency sweep. When a TLSD was used, two new natural frequencies formed above and below the first natural frequency of the tower. After installing the TLPD, the dynamic response of the test tower could be efficiently reduced at an excitation frequency in the range of the first natural frequency. The frequency band forms a wider plateau without pronounced maxima. While the installation of a TLSD increased the structural damping measured in free vibration tests from 0.14% to 0.95%, the installation of the TLPD leads to a significant increase to 6.48%. Further test series with varying mass ratios, increased excitation forces of the harmonic excitation in the frequency sweep and excitations at the tower head by white noises as force signals are planned. From the present results, a significant increase in damping and a reduction in the maximum amplitudes occurring can already be seen through the use of a TLPD. These optimised damping properties result in improved system responses of the structure under dynamic actions. It is possible to apply the TLPD to slender buildings under earthquake effects, as well as for masts and wind turbines under wind load. The use of the TLPD can significantly improve the fatigue behaviour and service life of slender structures in the presence of horizontal vibration.

Acknowledgements

The project on which this article is based was funded by the Federal Ministry of Education, and Research under the funding code 03THW03L02. The responsibility for the content of this publication lies with the author.

REFERENCES

[1] L. Stempniewski, B. Haag, *Baudynamik-Praxis: Mit zahlreichen Anwendungsbeispielen, 1st Edition.* Bauwerk, 2010.

[2] Ch. Petersen, Schwingungsdämpfer im Ingenieurbau. *Bautechnik, **79**,* 124-124, February, 2002.

[3] J.P. Den Hartog, *Mechanical Vibrations, 4th Edition, Reprint.* Dover Publications Inc., 1985.

[4] C. Verwiebe, *Grundlagen für den baupraktischen Einsatz von Schwingungsdämpfern auf Flüssigkeitsbasis.* Diss., Aachen, Techn. Hochschule, Shaker, 1998.

[5] E.W. Graham, A.M. Rodriguez, The characteristics of fuel motion which affect airplane dynamics. *Journal of Applied Mechanics,* ***19****,* 381-388, September, 1952.

[6] G.W. Warburton, Optimum absorber parameters for various combinations of response and excitation parameters. *Earthquake Engineering & Structural Dynamics,* ***10****,* 381-401, May/June, 1982.

[7] J. Krabbenhøft, *Shallow Water Tuned Liquid Dampers: Modeling, simulation and experiments.* Diss., Technical University of Denmark, May, 2011.

[8] H.F. Bauer, Oscillations of immiscible liquids in a rectangular container: A new damper for excited structures. *Journal of Sound and Vibration,* ***93****,* 117-133, March 8, 1984.

[9] R.A. Ibrahim, *Liquid Sloshing Dynamics-Theory and Applications.* Cambridge University Press, 2005.

[10] P. Warnitchai, T. Pinkaew, Modelling of liquid sloshing in rectangular tanks with flow-dampening devices. *Engineering Structures,* ***20****,* 593-600, July, 1998.

[11] M.J. Tait, Modelling and preliminary design of a structure-TLD system. *Engineering Structures,* ***30****,* 2644-2655, October, 2008.

[12] M. Péntek, A. Riedl, K.-U. Bletzinger, F. Weber, Investigating the Vibration Mitigation Efficiency of Tuned Sloshing Dampers Using a Two-Fluid CFD Approach. *Applied Sciences,* ***12****,* 7033, July, 2022.

[13] C. P. Wellmer, Design approach of the integration of a TLPD in small wind turbines. *Sketchbook,* ***unpublished*** Course work, University of Applied Sciences Wismar, Faculty of Design, July, 2022.